

# Similarity Test and Numerical Simulation on Deformation Failure of an Open-pit Slope under the Influences of Mining

Luo Xiao<sup>a</sup>, Junwen Zhang<sup>b</sup>

<sup>a</sup>China University of Mining & Technology (Beijing), College of Resources & Safety Engineering, Beijing 100083, China

<sup>b</sup>Heilongjiang University of Science and Technology, College of Mining Engineering, Haerbin 150022, China  
[luoxiao528@163.com](mailto:luoxiao528@163.com)

Underground mining significantly influences open-pit slope stability and threatens the overall slope safety as well as field safety production. This study discussed stress transfer characteristics in underground mining and the corresponding open-pit slope stability by combining a similarity model test and a numerical simulation on the Anjialing open-cast mine in Pingshuo, Shanxi. Thus, the position of terminal mining line was determined reasonably. The similarity model and numerical simulation results demonstrated that horizontal displacements of the slope free faces were approximately 2.2 and 2.3 m when the 29210 working face advanced to places 419 and 364 m away from the slope foot. The crack between the first and second steps of the slope was cut through and extended to downward steps when the working face approached the designed terminal mining line. As the working face advanced for another 60–120 m, the crack reached the slope foot and the upper steps rolled out. The reasonable terminal mining line 2 (364 m away from the slope foot) was the appropriate position to stop mining. Numerical calculation results were in high accordance with similarity model results. These research results have great significance in guiding the safety of open-pit mining.

## 1. Introduction

After open-cast work advances with increasing depth, the open-underground coordinated mining becomes the main mining method. Underground mining significantly influences the overall stability of an open-pit slope. Overlaying rock deformation and slope stability in an open-underground coordinated mining are the main constraints against open-underground combined mining (Sun et al., 2000). Open-underground coordinated mining can be simulated in laboratory with similar materials, through which unknown strata movement during the mining process (Sun et al., 1999; Zhang et al., 2012) and slope deformation parameters are obtained. Meanwhile, a numerical simulation can disclose the influence degree of underground mining on open-pit slope stability, and slope damages caused by underground mining can be predicted. The comparative analysis between a similarity model test and a numerical simulation provides a powerful guide to the field safety production of open-pit mines. Nowadays, only few studies concerning the influences of underground mining on open-pit slope stability are conducted. Therefore, the deformation failure mechanism of an open-pit slope during underground mining remains unclear. Further studies are needed to obtain a profound understanding of such mechanism and to provide accurate and reasonable solutions for specific field problems.

This study investigated the stress transfer characteristics in underground mining and the corresponding open-pit slope stability of Anjialing open-cast mine by combining the similarity model test and numerical simulation. Thus, the position of terminal mining line was determined reasonably, and the influences of underground mining on the deformation failure of an open-pit slope were concluded. The research results provided theoretical support for reasonable and safe field mining in open pits.

## 2. Similar material test model

### 2.1 Material ratio

The similar material model used a mixture of silica sand, calcium carbonate and gypsum as aggregate. The materials were mixed according to the specified compressive strength. Cement, lime, kaolin, paraffin and

distilled water with retarder were used for reinforcement. They were stirred evenly and then filled in the given moulds. The apparent density of the similar materials was 1.5 g/cm<sup>3</sup>, and the grain size of silica sand was limited between 50 and 100 meshes. Mica powder was applied for layering, and every filling thickness was generally 5–10 mm. The mixing ratio of silica sand, lime, gypsum and other similar materials (Yin et al., 2011) is listed in Table 1.

Table 1: Mixing ratio of similar materials

Layer no. (top own)	Lithology	Matching no.	Sand-Binder ratio	Cement		Water	Compressive Strength /MPa	
				Lime	Gypsum		Prototype	Model
1	Backfill	773	7:01	0.7	0.3	1:09	1.8	0.004
2	Loess	773	7:01	0.7	0.3	1:09	1.8	0.004
3	Weathered	455	4:01	0.5	0.5	1:09	56.3	0.125
4	Sandstone	355	3:01	0.5	0.5	1:09	95.1	0.211
5	Clay	637	6:01	0.3	0.7	1:09	58.1	0.129
6	4#coal seam	555	5:01	0.5	0.5	1:09	40.7	0.090
7	Sandy mudstone	637	6:01	0.3	0.7	1:09	63.8	0.142
8	Fine sandstone	437	4:01	0.3	0.7	1:09	99.4	0.221
9	Siltstone	437	4:01	0.3	0.7	1:09	107.4	0.239
10	Malmstone	455	4:01	0.5	0.5	1:09	54.4	0.121
11	9#coal seam	555	5:01	0.5	0.5	1:09	38.4	0.085
12	Mudstone	455	4:01	0.5	0.5	1:09	54.5	0.121
13	11#coal seam	555	5:01	0.5	0.5	1:09	36.6	0.081
14	Middle-fine sandstone	337	3:01	0.3	0.7	1:09	99.8	0.221

## 2.2 Monitoring point arrangement of the model

A BW-5 pressure cell was built firstly in the model to understand the distribution and variation of mining bearing stress with the advancement of working faces, and real-time stress monitoring was achieved with a YJZ-32A intelligent digital deformer. A total of 12 stress monitoring points was set at an interval of 100 m in the roof strata, which was 8 m away from the coal bed. The model test stand was 5000 mm(L) × 300mm(W) × 2000mm(H), and  $\alpha_L=250$ ,  $\alpha_t=15.8$  and  $\gamma_M=1.5\text{g/cm}^3$ ,  $\alpha_L=250$ . In the model test, apparent density and compressive strength were used as similarity indexes of the prototype and the model. Deformation, shear strength, elasticity modulus and Poisson's ratio were considered indirectly. The model was constrained on all sides. The front face was a free face, whereas the back face was horizontally restrained. The two sides of the model were closed during modelling based on the steel channel structure. The front and back faces of the model were shaped and reinforced with 100 mm-wide detachable steel channel plates. Given that the model was constrained on all sides, the initial ground stress status was simulated with a dead load of strata. Figure 1 shows the stress monitoring point arrangement of the model.



Figure 1: Stress monitoring point arrangement of the model.

## 3. Experimental analysis on stress transfer characteristics in underground mining

Figure 2 shows the results of stress monitoring data after the exploitation of 29210 working face. The reach of the advanced abutment pressure and position of the bearing stress peak is listed in Table 2. The 9#, 10# and 11# monitoring points were located horizontally on the stratum above the 29210-working face. According to the analysis on monitoring data, the stress reduction, stress increase and stress of primary rock zones were formed within a certain area of the overlying bed when the 29210-working face advanced. On the 29210-working surface, the stress concentration of the overlying bed increased firstly and then decreased gradually

as the distance to the coal wall increased. This observation was consistent with the distribution law of strata collapse and deformation (Hao et al., 2011). The stress in the slope rock mass increased sharply when the 29210-working face reached the designed terminal mining line. This finding indicated that the numerical value of the slope rock stress increased, and an evident stress concentration zone was formed. The continuous advancement of the 29210-working face resulted in the significant intensification of the stress concentration at the monitoring points on the slope, thereby reflecting that the numerical value of the slope rock stress soared. Slope deformation and breakage, and even the development of a glide plane or potential glide plane, were easily triggered under tensile and compressive stresses, which were serious threats against the stability of slope rock mass.

The deformation of the overlying bed during the advancement of the 29210-working face is shown in Figure 3. The crack in the slope rock mass was cut through when the 29210-working face approached the designed terminal mining line. This crack also extended to the downward steps. As the exploitation continued, this crack should be cut through completely. The crack extended to the slope foot when the 29210-working face advanced continuously after reaching the designed terminal mining line, and the upper slope rock mass nearly rolled out. Hence, whole slope sliding might occur. This observation implied that the working face should not be advanced any more for ideal results. Therefore, the terminal mining line was the appropriate position to stop mining.

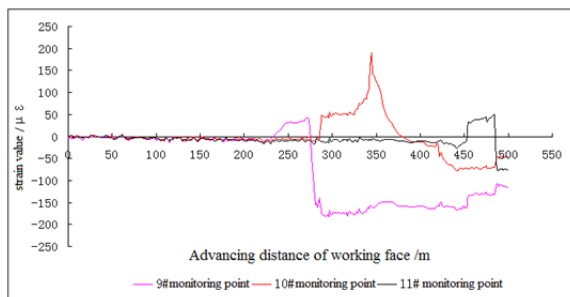


Figure 2: Variation curve of mining after the exploitation of the 29210-working face



(a) Working face advances to the place 486.5 m away from the slope foot (initial terminal mining line)



(b) Working face advances to the place 419 m away from the slope foot (reasonable terminal mining line 1)



(c) Working face advances to the place 364 m away from the slope foot (reasonable terminal mining line 2)



(d) Working face advances to the place 334 m away from the slope foot (designed terminal mining line)

Figure 3: Overlying bed deformation during the advancement of the 29210-working face

Table 2: Each of the advanced abutment pressure and position of the bearing stress peak

Monitoring point	Reach of the advanced abutment pressure /m	Position of the bearing stress peak (distance to the working face wall)/m
9	41	7.2
10	48	6.8
11	40	7.1

#### 4. Numerical simulation of the influence of mining on open-pit slope stability

Monitoring data on the positions and horizontal displacements of monitoring points on the slope are presented in Figure 4. A total of 15 monitoring points (1#–15#) were set top down on the slope. According to monitoring data analysis, the horizontal displacement of the slope (Liu et al., 2004; Song et al., 2012). Towards the free face increased continuously during the advancement of the 29210-working face. The horizontal displacement was approximately 1.8m when the 29210-working face reached the initial terminal mining line, thus showing a quick increasing tendency. Such horizontal displacement increased to approximately 2.2 and 2.3 m when the 29210-working face advanced to places 419 and 364 m away from the slope foot (reasonable terminal mining lines 1 and 2). Horizontal displacement during these two processes changed slowly. However, it increased dramatically as the designed terminal mining line was approached. If the working face advanced continuously, then horizontal displacement would increase accordingly. The cloud chart of the horizontal displacement showed that the crack between the first and second steps was cut through and was extended to the downward steps when the 29210-working face came close to the designed terminal mining line. This crack would extend further in the third step in the following mining activity. As the 29210-working face advanced for another 60–120 m, the crack extended to the slope foot and the upper steps were rolled out. Whole slope sliding might occur (Zhu et al., 2010; Yang et al., 2007). This observation reflected that the working face should stop advancing. According to the numerical simulation results, the reasonable terminal mining line 2 was the appropriate position to stop mining. This finding conformed to the test results of the similarity model.

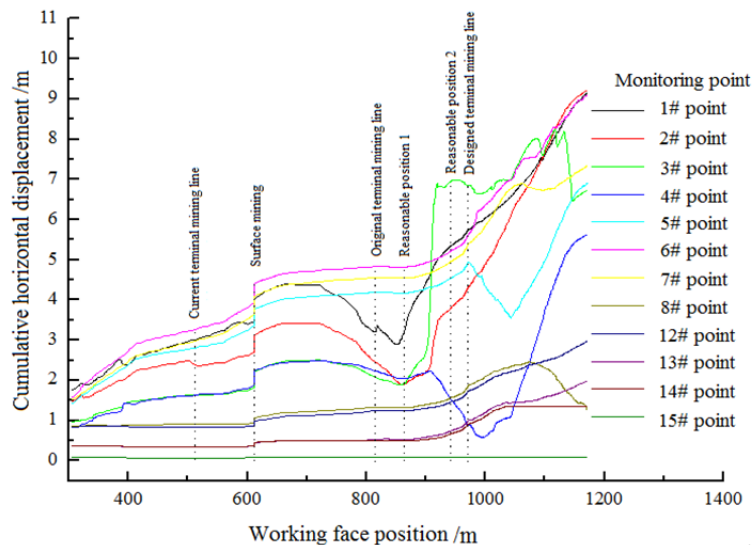


Figure 4: Monitoring data of the slope

Figure 5 shows the calculated horizontal displacement of the overlying bed (Han et al., 2006; Yao et al., 2013) in the continuous advancement of the working face after the designed terminal mining line. The ‘three zones’ on the overlying bed became increasingly evident as the working face advanced continuously. At the terminal mining line of the 4# coal bed, the 1390 flat plate subsided for approximately 0.5 m, and the slope between the 1380 flat plate and the 1345 flat plate had approximately 1.54 m horizontal displacement towards the free face. The cracks began to develop below the 1380 flat plate when the 29210-working face of the 9# coal bed advanced to the current terminal mining line, and the horizontal displacement between the 1380 flat plate and the 1345 flat plate was approximately 2.8 m. Subsequently, the free face of the 1360 flat plate tilted up, and cracks were observed below the 1360 flat plate. The horizontal displacement between the 1380 flat plate and the 1360 flat plate was approximately 4 m. The displacement changed in the same way when the 29210-working face of the 9# coal bed advanced to the initial terminal mining line (486.5 m away from the slope foot)

and the reasonable terminal mining line 1 (419 m away from the slope foot). The number of cracks below the 1360 flat plate increased, whereas the horizontal displacement of the slope between the 1380 flat plate and the 1360 flat slope was approximately 4.6 m. Horizontal displacement between the 1380 flat plate and the 1360 flat slope was approximately 5 m when the 29210-working face of the 9# coal bed advanced to the reasonable terminal mining line 2 (364 m away from the slope foot), and the displacement below the 1345 flat plate was approximately 2 m. The crack belt from the 1390 flat plate to the 1380 flat plate subsided (Wang et al., 2011; Zhai, 2012; Song et al., 2016) when the 29210-working face of the 9# coal bed advanced to the designed terminal mining line (334 m away from the slope foot), and the horizontal displacement between the 1380 flat plate and the 1360 flat slope was approximately 6 m. The displacement below the 1345 flat plate was approximately 2 m. If the working face advanced for another 60–120 m, the crack would extend to the slope foot and the upper steps might roll out. Therefore, the reasonable terminal mining line (364 m away from the slope foot) was the appropriate position to stop mining for the 29210-working face.

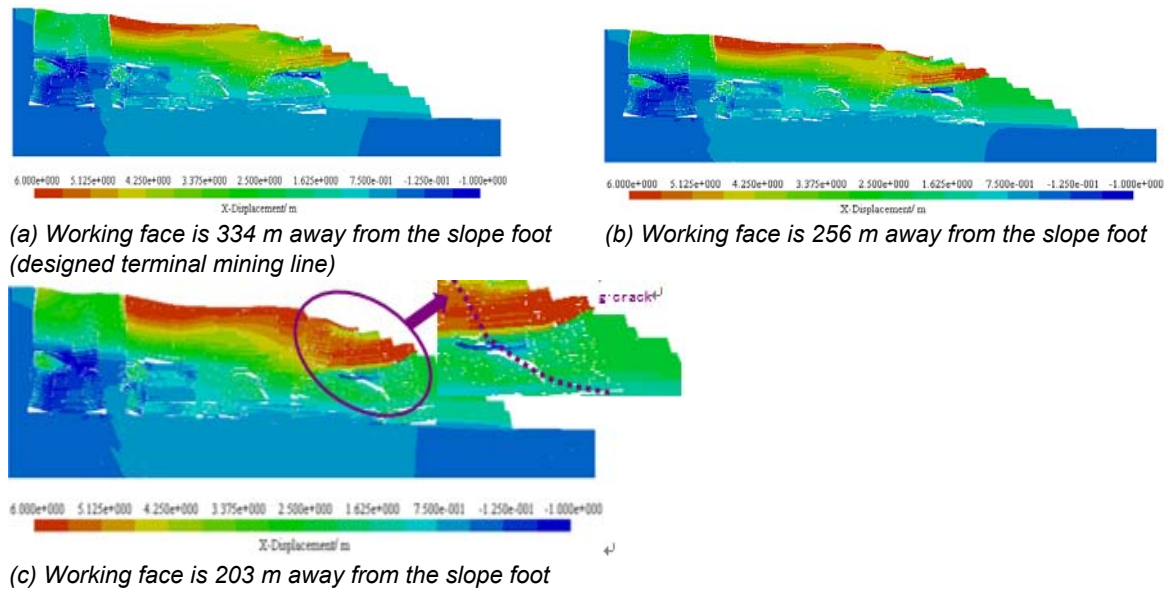


Figure 5: Calculated horizontal displacements

## 5. Conclusions

The following conclusions are obtained through the comparative analysis between the similarity test and the numerical simulation on deformation failure of an open-pit slope under open-underground combined mining:

- (1) According to the test result of the stress transfer characteristics in underground mining, the crack in the slope rock mass is cut through when the 29210-working face approaches the designed terminal mining line. In the mining that follows, the crack extends to the slope foot and the upper slope nearly rolls out. Hence, whole slope sliding may occur.
- (2) Based on the numerical analysis of the influences of underground mining on open-pit slope stability, the horizontal displacements towards the free face of the slope are approximately 2.2 and 2.3 m when the 29210 working face advances to places 419 and 364 m away from the slope foot. The crack between the first and the second steps of the slope is cut through and is extended to the downward steps when the working face approaches the designed terminal mining line. The crack reaches the slope foot as the working face advances for another 60–120 m and the upper steps roll out.
- (3) Both similarity test and numerical simulation conclude that the reasonable terminal mining line 2 (364 m away from the slope foot) is the appropriate position to stop mining for the 29210-working face. The research results provide powerful support for the safe mining of open pits.

## Acknowledgments

This work was supported by the Natural Science Foundation of China under Grant 51574114 and 51274122.

## Reference

- Chen S., Yang T., Zhang H., 2008, The slope stability under underground mining of Anjialing open-pit mine in Pingshuo, *Journal of China Coal Society*, 33(2), 148-152.
- Han F., Xie F., Wang J., 2006, 3-D numerical simulation on the stability of rocks in transferred underground mining from open-pit, *Journal of University of Science and Technology Beijing*, 28(6), 509-514.
- Hao G., Wu K., Li L., 2011, Similarity test system of Old goaf activation, *Coal Engineering*, 6, 74-76.
- Liu H., Chen W., Feng X., 2004, Numerical modeling of daye iron open-pit-mine transferring to underground mining by discrete element method, *Rock and Soil Mechanics*, 25(9), 1413-1417.
- Song J.X., Liu Y.F., Guo H.Y., Zhang S.W., 2016, Test and study on enhancement of coal reservoir permeability by autogenous nitrogen, *Chemical Engineering Transactions*, 51, 1045-1050, DOI: 10.3303/CET1651175.
- Song W., Fu J., Wang D., 2012, Study on physical and numerical simulation of failure laws of wall rock due to transformation from open-pit to underground mining, *Journal of China Coal Society*, 37(2), 186-191.
- Sun S., Cai M., Wang S., 1999, Effect of combined underground and open pit mining and deformation mechanism of slope, *Chinese Journal of Rock Mechanics and Engineering*, 18(5), 563-566.
- Sun S., Cai M., Wang S., 2000, Study of sliding mechanism for slope due to the excavation from open pit into underground mine, *Chinese Journal of Rock Mechanics and Engineering*, 19(1), 126-129.
- Wang Z., Hao Z., Shang W., 2011, Deep slope stability analysis and evaluation of Anjialing Open-pit north landslide area, *Mining Technique*, 11(3), 70-72.
- Yang Z., Yu X., Guo H., 2007, Study on catastrophe mechanism for roof strata in shallow seam longwall mining, *Chinese Journal of Geotechnical Engineering*, 29(12), 1763-1766.
- Yao H., You H., Fan Y., 2013, Study of sliding mechanism of Liujia'ao loess landslide, *Rock and Soil Mechanics*, 34(1), 182-188.
- Yin G., Li X., Wei Z., 2011, Similar simulation study of deformation and failure response features of slope and stope rocks, *Chinese Journal of Rock Mechanics and Engineering*, 30(Supp.1), 2913-2923.
- Zhai Z., 2012, Research on slopes instability mechanism and countermeasures of open-pit with underground plane coordinate mining, *Open Mining Technology*, 4, 4-6.
- Zhang J., Wu K., Ao J., 2012, Research on dynamical movement rule of overlying strata, *Coal mining Technology*, 17(2), 20-22.
- Zhao M., Sun X., Wang S., 2014, Damage Evolution Analysis and Pressure Prediction of Surrounding Rock of a Tunnel Based on Rock Mass Classification, *Electronic Journal of Geotechnical Engineering*, 19, 603-627. Available at [ejge.com](http://ejge.com).
- Zhu B., Li G., 2016, Experimental Simulation of the Mine Pressure in Chuancao Gedan Coal Mine, *Electronic Journal of Geotechnical Engineering*, 21, 1431-1444.
- Zhu J., Feng J., Peng X., 2010, The failure law of mine slope and the optimization of boundary parameter between open-pit and underground combined mining, *Journal of China Coal Society*, 35(7), 1089-1094.